nature physics

Supplementary information https://doi.org/10.1038/s41567-024-02643-5

Probing inhomogeneous cuprate superconductivity by terahertz Josephson echo spectroscopy

In the format provided by the authors and unedited

Supplemental Information

S1. Experimental Setup

A schematic of the 2-D terahertz spectroscopy experiment described in the Methods section is shown below in Fig. S1. Characterization of the two terahertz excitation pulses are shown in Fig. S2.

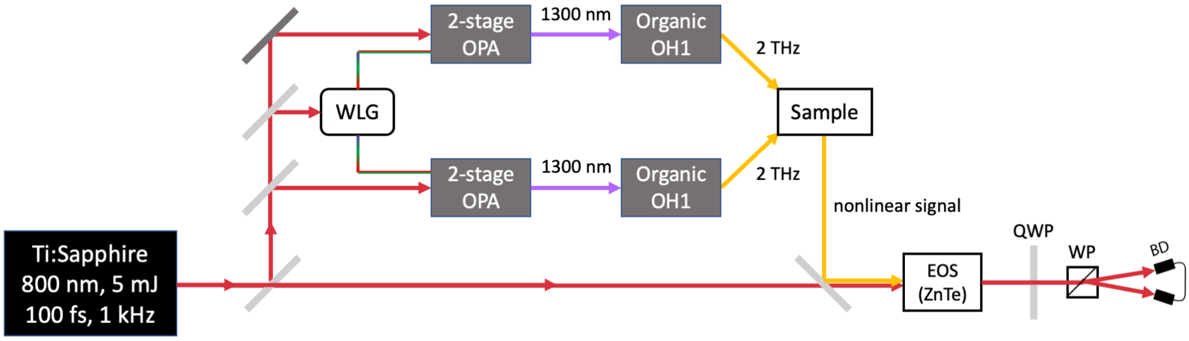

Fig. S1. Schematic of the optical set-up for 2-D terahertz spectroscopy, beginning with a commercial Ti:Sapphire amplifier. The labeling of the components is as follows: WLG = white-light generation, OPA = optical parametric amplifier, WP = Wollaston prism, BD = balanced detector, and QWP = quarter-wave plate.

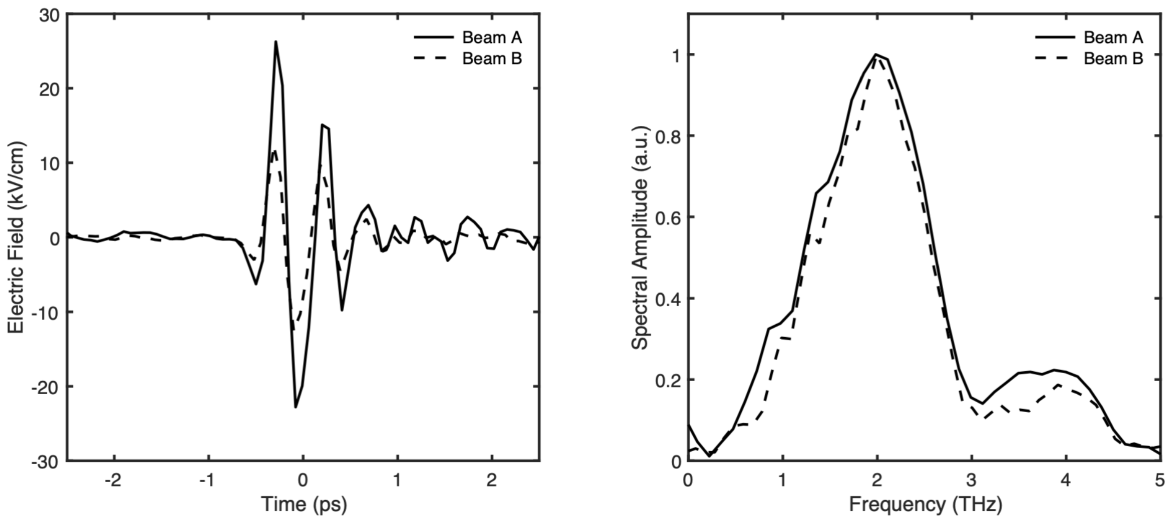

Fig. S2. Characterization of the two excitation pulses in time (left) and frequency (right).

S2. Dependence of Phase-Matching on Excitation Pulse Time-Ordering

Due to the non-collinear excitation geometry used here, the two excitation pulses are no longer equivalent and their time-ordering changes the phase-matching condition. In Fig. S3, we illustrate the phase-matching conditions for both pulse time-orderings:

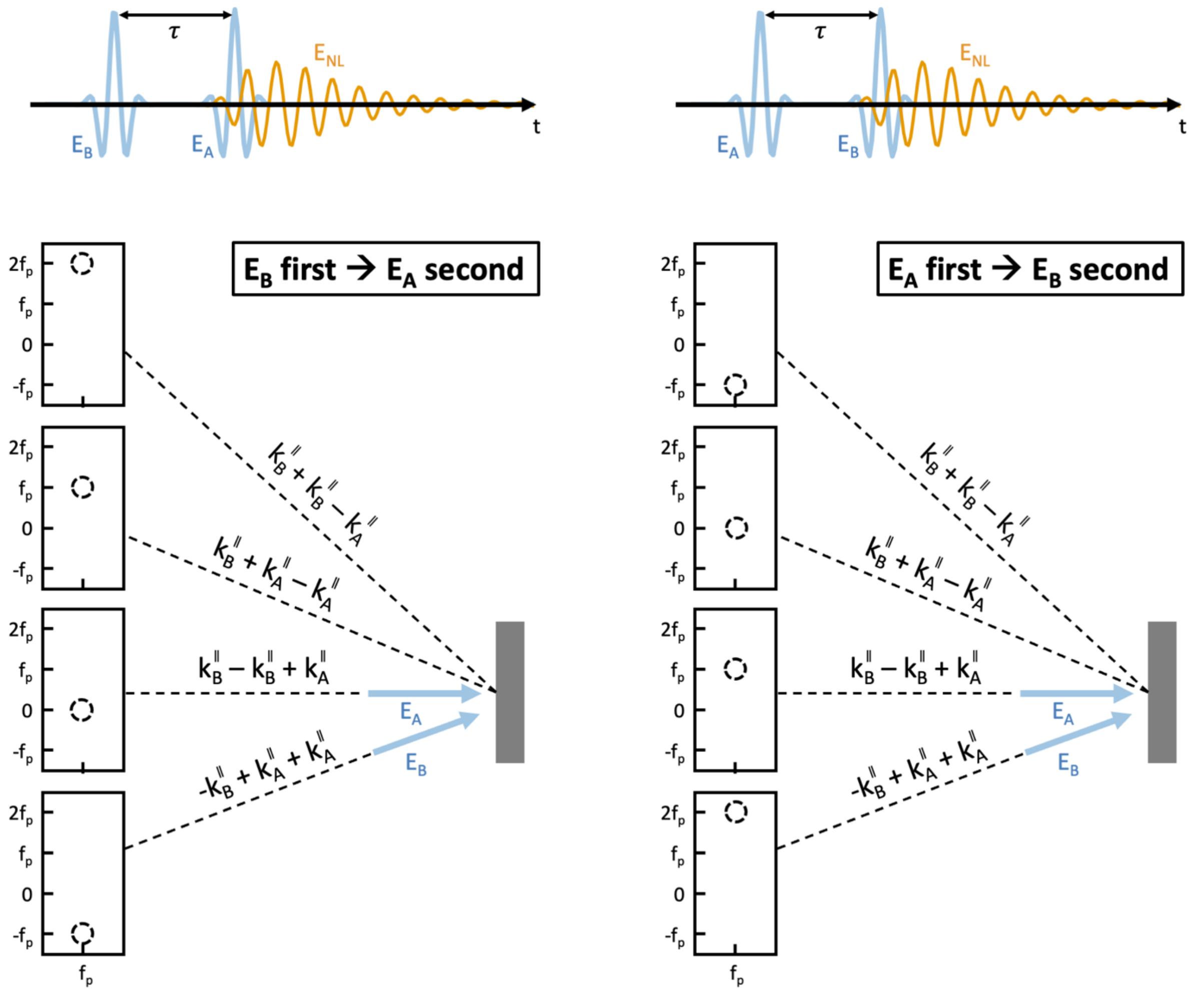

Fig. S3. Wavevector phase-matching conditions for the two possible time-orderings. (Left) E_B interacts with the sample first at an angle and (right) E_A interacts with the sample first at normal incidence.

We may further clarify the effect of time-ordering by first ignoring the E_A and E_B labels for the physical excitation fields, and considering the physical process that leads to, as an example, the $(f_t,f_\tau) = (f_p,0)$ peak nonlinearity. The position at zero along the vertical frequency axis (the conjugate axis of the inter-pulse time delay) indicates that no phase evolution occurs after the system interacts with the first excitation pulse, which we can call E_{first} for generality. This interaction is necessarily of the form $E_{first}E_{first}^*$ so that the excitation phases cancel and a rectified (zero-frequency) response results. The final nonlinear signal emission at f_p is then stimulated by a final interaction with the second excitation pulse E_{second}, which returns a total field scaling $E_{first}E_{first}^{*}E_{second}$. In the left panel of Fig. S3 E_B interacts with the material first, resulting in a field scaling $E_BE_B^{*}E_A$, while in the right panel of Fig. S3 E_A interacts with the material first, resulting in a field scaling $E_AE_A^{*}E_B$. The other phase-matching conditions may be understood in the same way.

S3. Comparison to Simulation

To verify the extracted parameters from our lineshape fits, namely $\gamma_{disorder}$ and $\gamma_{intrinsic}$, we simulate the expected Josephson echo signal given these parameters. Comparison of the experimental data and simulation at 6 K are shown in Fig. S4, in which excellent agreement is found in both the time and frequency domains.

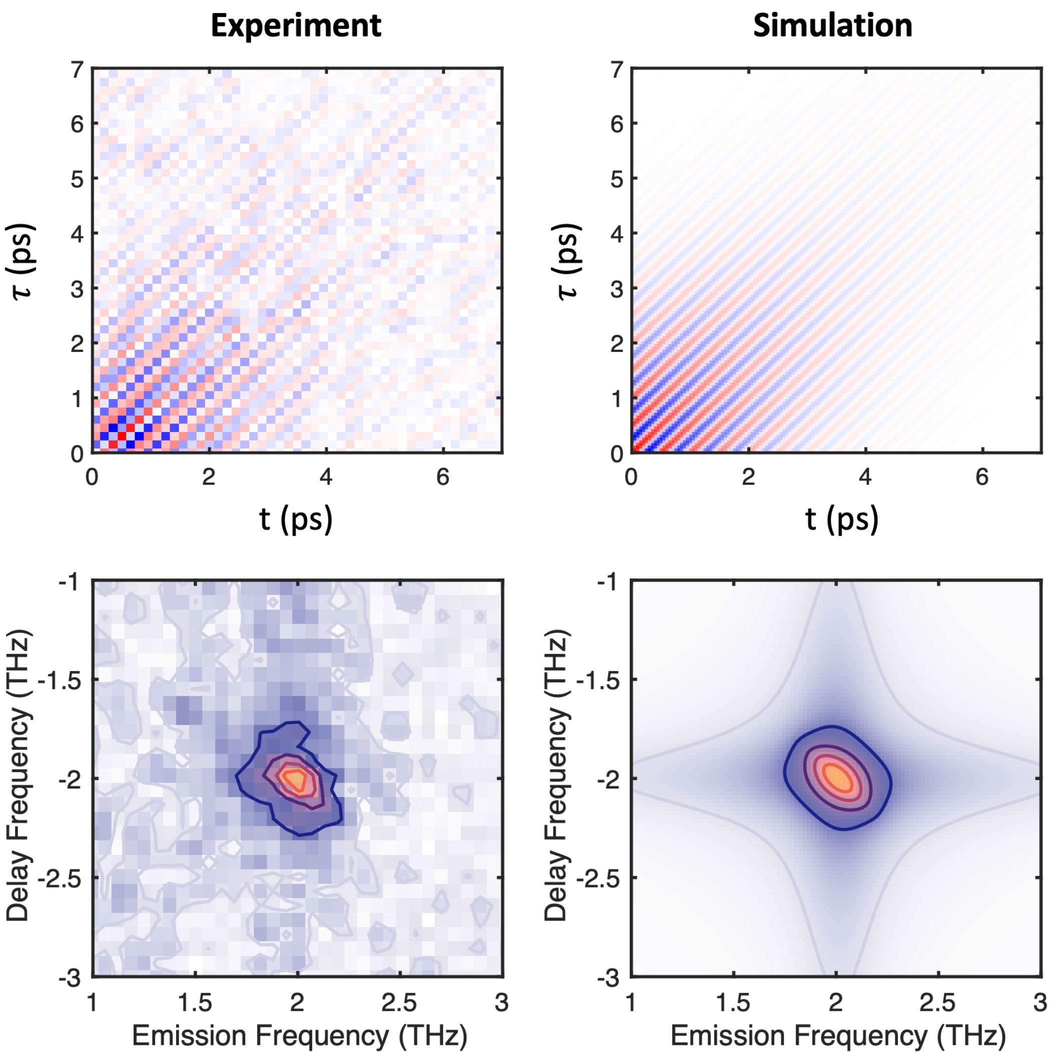

Fig. S4. Nonlinear Josephson echo signal measured by experiment (left) and simulated by the analytical solutions given in [1]. Characteristic echo contours are observed in both experiment and simulation, namely along $\tau = t$ in the time-domain and along $|f_t| = |f_\tau|$ in the frequency domain.

S3. Lineshape Functional Forms

The functional forms of the 'diagonal' and 'anti-diagonal' lineshapes as defined in the text are as follows:

$$S(\omega_{\tau'}) \propto \frac{\exp\left[\frac{(\gamma_{intrinsic} - i\omega_{\tau'})^2}{2\gamma_{disorder}{}^2}\right]\left\{\mathrm{Erfc}\left[\frac{\gamma_{intrinsic} - i\omega_{\tau'}}{\sqrt{2}\gamma_{disorder}}\right] + \exp\left[\frac{2i\gamma_{intrinsic}\omega_{\tau'}}{\gamma_{disorder}{}^2}\right]\mathrm{Erfc}\left[\frac{\gamma_{intrinsic} + i\omega_{\tau'}}{\sqrt{2}\gamma_{disorder}}\right]\right\}}{\gamma_{intrinsic}\gamma_{disorder}}$$

$$S(\omega_{t'}) \propto \frac{\exp\left[\frac{(\gamma_{intrinsic} - i\omega_{t'})^2}{2\gamma_{disorder}{}^2}\right]\mathrm{Erfc}\left[\frac{\gamma_{intrinsic} - i\omega_{t'}}{\sqrt{2}\gamma_{disorder}}\right]}{\gamma_{disorder}(\gamma_{intrinsic} - i\omega_{t'})}$$

Where the frequency axes are defined:

$$\omega_{t'} = (\omega_t + \omega_\tau)/2 \qquad \omega_{\tau'} = (\omega_t - \omega_\tau)/2$$

Details of the derivation for the above functional forms are given by Siemens et al. [1], and we only point out here that these fitting forms are derived by integrating a disordered ensemble of two-level oscillators over a distribution of resonance frequencies. We have found this expression to be valid after incorporating the dispersion of a many-body excitation [4], and it is directly analogous to the linear optical response functional form of a disordered JPR as an integral over a distribution of Josephson couplings (derived in [4]) applied by Dordevic et al. [5].

S4. Different Regimes of Relative Disorder

The two most intuitive cases for disorder are the limiting cases of zero disorder ($\gamma_{\mathrm{disorder}} = 0$) and dominant disorder ($\gamma_{\mathrm{disorder}} > \gamma_{\mathrm{intrinsic}}$). In the optimally-doped LSCO studied here however, disorder is subtle and $\gamma_{\mathrm{disorder}}$ is only a fraction of $\gamma_{\mathrm{intrinsic}}$. One can understand the shape of our observed 2-D spectra by interpolating between the two limiting cases described above.

One sees in the simulations presented in Fig. S5 that for the case of no disorder (left spectrum) a symmetric lineshape is observed, while for the case of dominant disorder (right spectrum) a stripe-like spectrum is observed which reflects the large JPR frequency distribution. The case of weak disorder (middle spectrum) that mimics optimally-doped LSCO therefore returns a lineshape that is an intermediate between the symmetric star-shaped spectrum and the stripe-like spectrum.

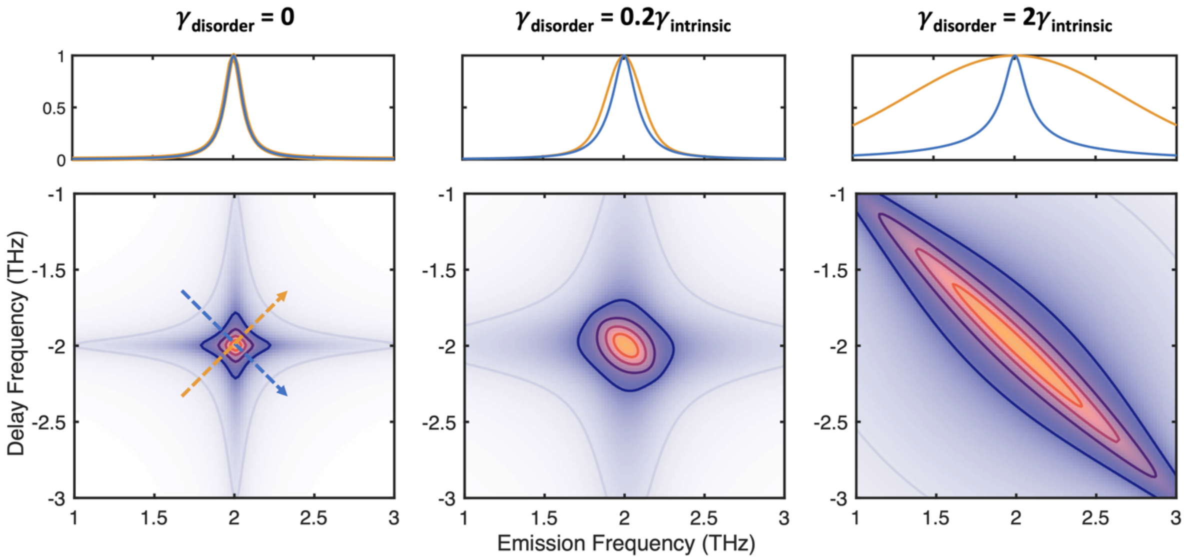

Fig. S5. Simulated Josephson echo spectra for three regimes of relative disorder: (left) no disorder, (middle) $\gamma_{disorder} < \gamma_{intrinsic}$, and (right) $\gamma_{disorder} > \gamma_{intrinsic}$.

S6. Disordered Reflectivity

As discussed in the main text, a model for inhomogeneous superconductivity incorporating a distribution of Josephson couplings was proposed by van der Marel & Tsvetkov [5] and successfully implemented by Dordevic et al. [6] to interpret distorted reflectivity profiles in LSCO. In Fig. S4, simulations of the reflectivity and loss function according to this model are presented for two values of $\gamma_{disorder}$, $\gamma_{disorder} = 0$ (no disorder) and $\gamma_{disorder} = 80$ GHz (the value derived in section S4 that agrees with the Josephson echo measurements). The fitted values from [6] (at x = 0.17 doping) for the normal and superfluid plasma frequencies ω_n and ω_p as well as the normal fluid scattering rate γ_{sr} rate were used.

One sees that, for this degree of inhomogeneous broadening, the homogeneous and disordered reflectivity differ only by a maximum of 2%. An anomalous peak is observed in the optical conductivity due to the presence of disorder, but with a relative amplitude on the order of 1%. Such a peak has been used as an indication of the presence of disordered superconductivity, but is only clearly observable in the limit of strong inhomogeneity [5].

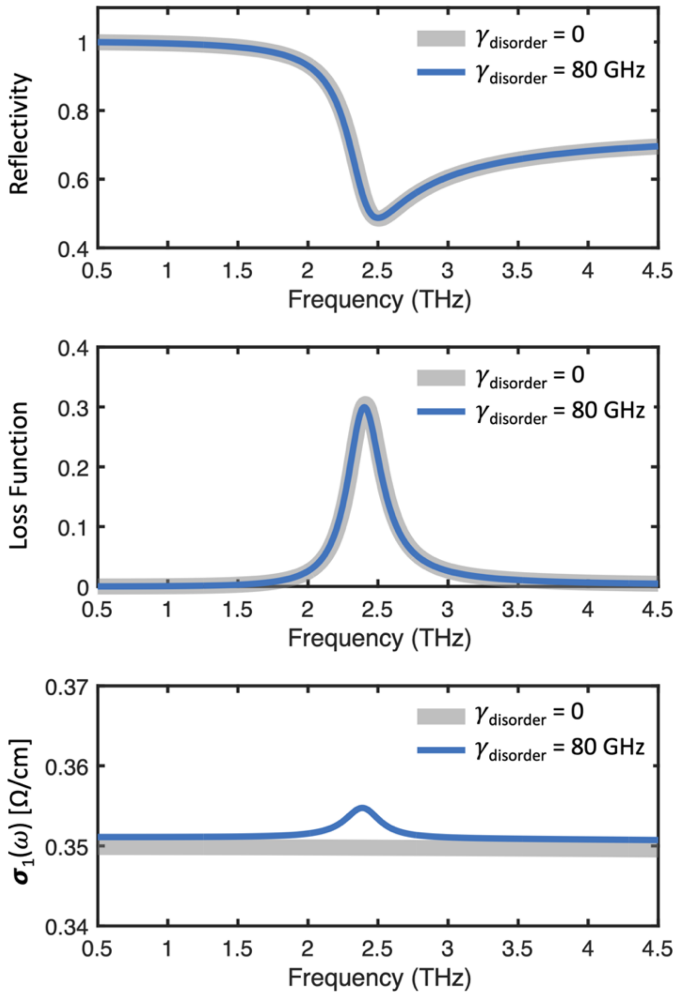

Fig. S6. Simulated reflectivity (top), loss function (middle), and optical conductivity (bottom) for homogeneous

References

[1] Siemens, M. E., Moody, G., Li, H., Bristow, A. D. & Cundiff, S. T. Resonance lineshapes in two-dimensional Fourier transform spectroscopy. *Opt. Expr.* **18**, 17699-17708 (2010).

[2] Koshelev, A. E. & Bulaevskii, L. N. Fluctuation broadening of the plasma resonance line in the vortex liquid state of layered superconductors. *Phys. Rev. B* **60** (1999).

[3] Kato, T., Okitsu, S. & Sakata, H. Inhomogeneous electronic states of La2-xSrxCuO4 probed by scanning tunneling spectroscopy. *Phys. Rev. B* **72** (2005).

[4] Salvador, A. G., Dolgirev, P. E., Michael, M. H., Liu, A, Pavicevic, D., Fechner, M., Cavalleri, A. & Demler, E. Principles of 2D terahertz spectroscopy of collective excitations: the case of Josephson plasmons in layered superconductors. arXiV:2401.05503.

[5] van der Marel, D. & Tsvetkov, A. Transverse optical plasmons in layered superconductors. *Czech. J. Phys.* **46**, (1996).

[6] Dordevic, S. V., Komiya, S., Ando, Y. & Basov, D. N. Josephson Plasmon and Inhomogeneous Superconducting State in $La_{2-x}Sr_xCuO_4$. *Phys. Rev. Lett.* **91**, 16 (2003).